WA-3 10:20

Proceedings of the 33rd
Conference on Decision and Control
Lake Buena Vista, FL - December 1994

Improving Static Performance Robustness of Thermal Processes*

M. Güntekin Kabuli and **Robert L. Kosut**
Integrated Systems Inc.
3260 Jay Street, Santa Clara, CA 95054-3309
kabuli@isi.com, kosut@isi.com

Stephen Boyd
Information Systems Laboratory
Stanford University, Stanford, CA 94305
boyd@isl.stanford.edu

Abstract

A static (steady-state) robust control design problem is considered using a nonlinear model of a thermal system. For a given operating point, the control problem is to determine a feedforward/feedback static controller that minimizes the worst-case static peak performance deviation from nominal in the presence of bounded disturbances and parameter variations. It is desired to obtain the tradeoff between the size of the worst-case deviation and the size of the uncertainty set. A complete solution is derived for the static linear control design problem obtained from linearization about selected operating points. Efficient computational tools are developed to rapidly analyze numerous operating points and control configurations.

1 Introduction

Rapid thermal processing (RTP) systems demand fast tracking control laws that achieve near uniform spatial temperature distributions across the target, e.g., a semiconductor wafer, during both transient and steady-state phases of the process.

In this paper we only address the static (steady-state) problem using static feedforward/feedback control laws. The approach relies on a static nonlinear heat transfer model which includes parameter uncertainty. The form of the model found to be very convenient for robust control design is obtained by forming a mesh of branches that model conduction, convection and radiation between the nodes of the mesh. A systematic modeling approach based on the analysis of large scale nonlinear resistive networks can then be applied to obtain the equations that determine the operating points in terms of input and disturbance biases. This model structure is generic, since all thermal system models can be put in this form [1, 2] .

For a given operating point, the control problem is posed as designing a feedforward/feedback static controller that minimizes the worst-case peak deviation of the performance variables from a nominal point when subjected to bounded disturbances and parameter variations. Since the solution to this nonlinear problem is not known, a sequence of approximations in terms of the small-signal equivalents are used to pose static linear control problems. We derive a complete solution to the associated static linear control design problem. Considering problem sizes of interest, (e.g., 20 actuators, 20 sensors, 100 regulated variables, 100 exogenous disturbances) , efficient computational solution methods are investigated and prototype tools are developed to simplify comparative design studies resulting from different choices of operating points, actuators, sensors and control laws (feedforward and/or feedback).

The paper is organized as follows: in Section 2 we pose and solve the static linear *sensitivity* problem, i.e., parameter uncertainties are included as additional exogenous input perturbations. The tools required here are also needed for the robustness problem. An example of the sensitivity tradeoffs using the thermal mesh model is given in Section 3. Robustness results for real parametric uncertainties are given in Section 4. An example, using the developed tools, is given in Section 5. To conserve space, only a very brief discussion of the computational issues and methods is provided. Further details on the optimization methods and proofs can be obtained from the authors.

2 Sensitivity Tradeoff

2.1 Problem Description

Consider the feedback interconnection shown in Figure 1 , where w, z, u and y denote the exogenous inputs, controlled outputs, actuator inputs and measured outputs, respectively; $P \in \mathbb{R}^{(n_z+n_y)\times(n_w+n_u)}$ denotes a static linear plant, $K \in \mathbb{R}^{n_u \times n_y}$ denotes a static linear feedback controller, and $u_K \in \mathbb{R}^{n_u}$ denotes the static feedforward control.

*Research supported by ARPA under AFOSR contract F49620-94-C-0003 and Army Missile Command contract DAAH01-93-C-R193.

0-7803-1968-0/94$4.00©1994 IEEE

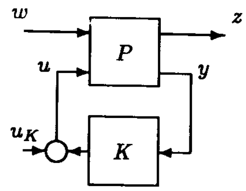

Figure 1: Static feedback system

To address the sensitivity to parameter variation, the exogenous input w includes disturbances as well as parameter perturbations from nominal. As such it is convenient to explicitly account for the nominal as well as deviations. Hence, let the normalized exogenous input be given by

$$\eta_w = \Delta_w^{-1}(w - w_0)$$

where $w_0 \in \mathbb{R}^{n_w}$ is the nominal value and Δ_w is a diagonal scaling matrix. A normalized output η_z is defined accordingly:

$$\eta_z = \Delta_z^{-1}(z - z_0) \quad .$$

Motivated by the temperature uniformity requirements of RTP problems, we are naturally led to consider the "infinity" norm as the appropriate measure of signal size. Thus, for $x \in \mathbb{R}^n$, the infinity norm is defined as $||x||_\infty = \max_{1 \le k \le n} |x_k|$. Recall also that the induced matrix norm is the "max-row-sum", i.e.,

$$||A||_{i,\infty} = \max_{||x||_\infty \le 1} ||Ax||_\infty = \max_i \sum_j |a_{ij}| \quad .$$

We can now state the fundamental design problem:

- **Optimal Design Tradeoff:** For a given P, w_0, z_0 , Δ_w, and Δ_z, find the optimal tradeoff between disturbance size $||\eta_w||_\infty$ and performance tolerance $||\eta_z||_\infty$, i.e., determine the graph:

$$\begin{array}{c} \{(\lambda_w \ , \lambda_z) \mid \lambda_w \ge 0\} \\ \lambda_z = \min\limits_{(K,u_K)} \max\limits_{||\eta_w||_\infty \le \lambda_w} ||\eta_z||_\infty \end{array} \tag{1}$$

The graph in (1) of λ_z vs. λ_w gives the minimum relative change (λ_z) uniformly in all performance variables (z) for a relative uniform change (λ_w) in all exogenous input variables (w). Hence, the graph denotes the ***boundary*** between feasible and infeasible designs on the $(\lambda_w, \lambda_z)-$ plane. A typical tradeoff curve – the graph described in (1) – is shown by the solid line in Figure 2. The shaded region below this tradeoff curve is infeasible, i.e., there exists no combination of feedforward or feedback which can achieve the requested performance. Conversely, all $(1, 1)-$feasible designs correspond to points on the segment between designs **A** and **B** in Figure 2 . Note that **A** corresponds to a performance design and **C** corresponds to a robust design, i.e., design **C** allows a much larger uncertainty for the requested specification $||\eta_z||_\infty \le \lambda_z = 1$. In general, the graph that partitions the feasible and infeasible regions is neither convex nor concave.

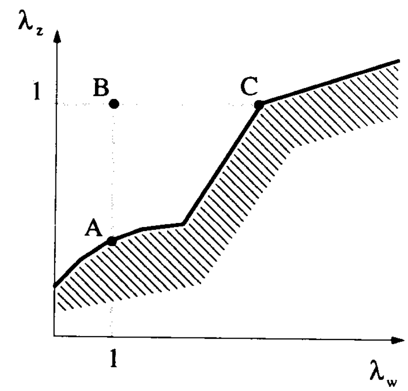

Figure 2: Graph in (1) denoting the boundary of the feasible region in the (λ_w,λ_z)-plane; shaded region is infeasible.

Due to the two free design parameters K and u_K , four possible problems can be posed, namely:

- open-loop ($u = 0$),
- feedforward only ($u = u_K$),
- feedback only ($u = Ky$),
- feedforward/feedback ($u = u_K + Ky$) .

Typical design specifications involve the following:

- feasibility: determine (if possible) a $(\lambda_w, \lambda_z)-$feasible design
- robustness: for a fixed λ_z, maximize λ_w among $(\lambda_w, \lambda_z)-$feasible designs
- performance: for a fixed λ_w, minimize λ_z among $(\lambda_w, \lambda_z)-$feasible designs.

The feasibility, robustness and performance design problems stated above can all be expressed in terms of the tradeoff curve denoted by the graph in (1) . In fact, it can be shown that the four possible choices of control ($u = 0$, $u = Ky$, $u = u_K$, $u = u_K + Ky$) result in special cases of finding a solution to a problem of a max-row-sum norm minimization of the form:

$$\min_X ||T_1 + T_2 X T_3||_{i,\infty} \quad . \tag{2}$$

where the T's and X are defined in accordance with the four cases.

2.2 Positive Definite Programming

To efficiently solve the above max-row-sum problem we utilise the primal-dual potential reduction methods described in [4]. The computational tools we have developed resolve the following difficulties: 1) Initialization of primal and dual variables ; 2) Efficient approximate solutions to the (huge) least-squares problems to determine the analytic center ; 3) Perturbation of the updated dual parameters. To further explain these very important but esoteric issues is outside the scope for this paper. Interested readers can request details from the authors. For the intended applications $(n_z n_w) \gg (n_u n_y) \gg 1$. The particular solution approach reduces the original $(n_z n_w + n_w + n_u n_y + n_u + 1)$-unknown least-squares problem to a $(n_u n_y + n_u)$-unknown least-squares problem. Hence the computational complexity is determined by the control variables: $(n_u n_y)$ for feedback and n_u for feedforward.

3 Example: Sensitivity Tradeoff

The mesh in Figure 3 represents a resistive network consisting of seven nodes and nine branches. The mesh describes conduction, convection and radiation effects as non-linear resistive elements. (The authors have used an *Xmath* script to automate the mesh generation and the associated linearised model at the steady-state.) Following standard node analysis results for linear resistive networks (see e.g. [1]) , the steady-state heat-flux conservation equations arising from application of the Kirchhoff Current Law at each and every node (except the reference (datum) node) result in:

$$0 = A_c G A_c^T x + A_u u + A_w w, \quad y = Cx \quad . \qquad (3)$$

The node variables x correspond to node temperature minus the ambient temperature, u denotes the control input fluxes, and w the disturbance fluxes. The measured node temperatures are denoted by y . The matrix $[A_c \ A_u \ A_w]$ is defined by the incidence matrix that describes the interconnection of branches; its entries are 0's, 1's or -1's . The matrix G is diagonal consisting of nominal branch conductances. For this example, the regulated variables are chosen as the six node temperatures. Hence, $n_w = 2$, $n_u = 2$, $n_z = 6$ and $n_y = 2$. Thus $P \in \mathbb{R}^{8\times4}$, $K \in \mathbb{R}^{2\times2}$ and $u_K \in \mathbb{R}^2$. We seek at most $n_u(n_y+1) = 6$ control variables and introduce $n_z(n_w+1)+1 = 19$ slack variables. Following the notation in Section 2 , let $w_{0,i} = 1, i = 1,2$; $\Delta_w = I$; $z_{0,i} = 3, i = 1,\ldots,6$; $\Delta_z = I$.

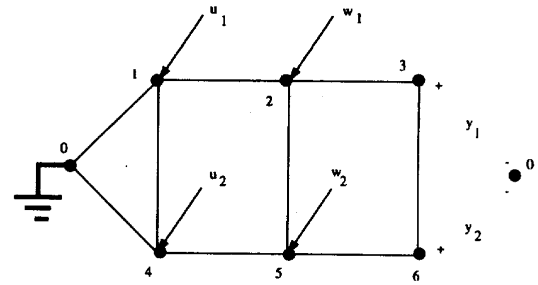

Figure 3: Sample mesh

The tradeoff curve in (1) is derived for five cases (see Figure 4) . One extra design approach is introduced to illustrate that the feedforward and feedback designs are not decoupled. In other words, minimizing over u_K for $K = 0$ and then fixing the optimal u_K value and then optimizing over K is not equivalent to the simultaneous minimization over u_K and K .

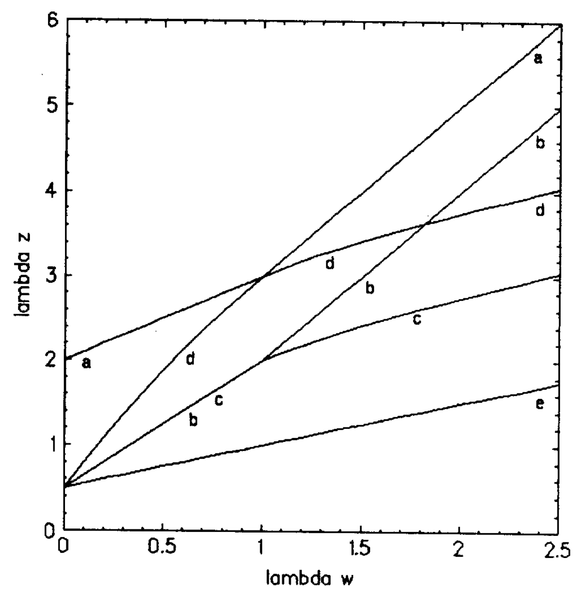

Figure 4: Tradeoff curves in (1) for the five cases:
a – open-loop
b – feedforward only
c – one at a time optimization: first feedforward and then feedback
d – feedback only
e – simultaneous optimization: feedforward and feedback

4 Robustness Analysis

The control design problem formulated in Section 2 is based on a nominal plant model $P : (w, u) \mapsto (z, y)$, where w includes perturbations in uncertain parameters. In this section, we consider the performance of the nominal control $u = u_K + Ky$ subject to perturbed plant models as shown in Figure 5 , where w now includes only exogenous disturbances.

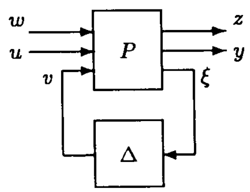

Figure 5: Perturbed plant model

Although we still consider linearized plant models, the uncertainty is maintained in its natural form (Figure 5) . In the example to follow we take Δ as a diagonal matrix whose entries correspond to uncertainties in the branch conductance matrix G . Hence, the perturbed form of the linear resistive network (3) becomes:

$$0 = A_c(G + \Delta)A_c^T x + A_u u + A_w w \quad . \qquad (4)$$

In order to define the uncertainty set, let e_i denote the ith standard basis vector. Its dimension is determined from the context. Now, the uncertainty structure and vertex set are defined as follows:

$$\mathcal{D} = \{\Delta \in \mathbb{R}^{n_v \times n_\xi} \mid \Delta_l \leq \Delta \leq \Delta_u\} \quad , \qquad (5)$$

$$\mathcal{V}_\mathcal{D} = \{\Delta \in \mathcal{D} \quad | \quad e_i^T \Delta e_j \in \{e_i^T \Delta_l e_j, e_i^T \Delta_u e_j\}, \; 1 \leq i \leq n_v \;, \; 1 \leq j \leq n_\xi \} \quad . (6)$$

Let $H_{zw}(\Delta)$ denote the fractional form obtained for $u = Ky$ (for $u = u_K + Ky$, w gets augmented by one entry) . From Figure 5,

$$H_{zw}(\Delta) = H_{11} + H_{12}\Delta(I - H_{22}\Delta)^{-1}H_{21} \quad .$$

Let $\det(I - H_{22}\Delta) \neq 0$ for all $\Delta \in \mathcal{D}$. Under these assumptions, it can be shown that:

$$\max_{\Delta \in \mathcal{D}} \|H_{zw}(\Delta)\|_{i,\infty} \;=\; \max_{\Delta \in \mathcal{V}_\mathcal{D}} \|H_{zw}(\Delta)\|_{i,\infty} \quad . \qquad (7)$$

This result means that the worst-case maximum row sum of the linear fractional form $H_{zw}(\Delta)$ over $\mathcal{D}$ is achieved at the vertex set $\mathcal{V}_\mathcal{D}$. We utilize this result in the following section, in a design example. It can also be shown that $\min_{\Delta \in \mathcal{D}} \|H_{zw}(\Delta)\|_{i,\infty}$ is not necessarily achieved at the vertex set.

5 Example: Robustness Analysis

We consider a mesh consisting of 40 linear conductance branches and 25 temperature nodes. As in (3) , $[A_c, A_u, A_w] \in \mathbb{R}^{24 \times (40+5+3)}$ is the incidence matrix and consists of 0's, 1's and -1's to denote the directed graph associated with the mesh. $u \in \mathbb{R}^5$ and $w \in \mathbb{R}^3$ denote the control input and exogenous input fluxes, respectively. $y \in \mathbb{R}^5$ denotes the measured node temperatures. The node temperatures satisfy (3) where $G = \mathrm{diag}(g)$. Nominal operating conditions (denoted by 0 subscripts) are determined to minimize the deviation from a uniform temperature profile across the measured nodes. The nominal operation is determined by

$$A_c \;\mathrm{diag}(g_0)\; A_c^T x_0 + A_u u_0 + A_w w_0 = 0 \quad ,$$

where $g_0 > 0$ and $w_0 > 0$. Let the performance variable z be defined as $z = [y^T \; u^T]^T$, where $z_0 > 0$. The design problem is posed as follows: determine $u = u_K + Ky$ such that the performance measure

$$\varphi(u_K, K) = \max_{\substack{\|\Delta_w^{-1}(w - w_0)\|_\infty \leq 1 \\ \|\Delta_G^{-1}(g - g_0)\|_\infty \leq 1}} \|\Delta_z^{-1}(z - z_0)\|_\infty$$

is minimized for the feedback perturbed plant model in Figure 5 ; we choose $\Delta_w = \mathrm{diag}(w_0)$, $\Delta_G = 0.1\mathrm{diag}(g_0)$ and $\Delta_z = \mathrm{diag}(z_0)$. Recall that by (7) , the performance measure is achieved at the vertices. Note that we allow a 10% uncertainty in all 40 conductance branches. Hence, for a given design, the exact measure could have been obtained by 2^{40} max row sum evaluations. To make the calculations reasonable, we will rate the designs according to 10% uncertainty in the ***first*** 10 conductance branches; hence determine a lower bound on φ (but this is exact if only 10 parameters are varied) .

In the first design approach, we take $G = G_0$ and solve

$$(u_{K_1}, K_1) = \arg \min_{(u_K, K)} \max_{\substack{\|\Delta_w^{-1}(w - w_0)\|_\infty \leq 1 \\ G = G_0}} \|\Delta_z^{-1}(z - z_0)\|_\infty \; .$$

Thus, the control law is optimal under perfect plant modeling.

In the second design approach, the first order approximation to the plant

$$A_c \;\mathrm{diag}(g_0)\; A_c^T(x - x_0) + A_u(u - u_0) + A_w(w - w_0) + A_c \;\mathrm{diag}(g - g_0)\; A_c^T x_0 \;=\; 0 \qquad (8)$$

is used to solve for the optimal sensitivity controller

$$(u_{K_2}, K_2) = \arg \min_{(u_K, K)} \max_{\substack{\|\Delta_w^{-1}(w - w_0)\|_\infty \leq 1 \\ \|\Delta_G^{-1}(g - g_0)\|_\infty \leq 1}} \|\Delta_z^{-1}(z - z_0)\|_\infty \; .$$

In other words, the input to the Δ block in Figure 5 is fixed at $\xi_0 = A_c^T x_0$, and the exogenous inputs w are augmented by 40 more entries to account for $(g - g_0)$ in (8). The results are summarized in Table 1.

	$g = g_0$	$0.9g_0 \leq g \leq 1.1g_0$
$\varphi(u_0, 0)$	6.99%	$\geq$ 13.37%
$\varphi(u_{K_1}, K_1)$	3.47%	$\geq$ 223.45%
$\varphi(u_{K_2}, K_2)$	3.67%	$\geq$ 6.63%

Table 1: Performance ratings

Note that the first row in Table 1 corresponds to the openloop performance. The input is set to u_0 ; hence the performance measure reflects the relative change in y about y_0 . At the nominal conductance parameters, worst-case deviation is 6.99% and when the first 10 conductances have 10% uncertainty, worst-case deviation is 13.37% . Note that the second column of Table 1 is a lower bound on the performance measure φ since the parameter perturbations are restricted to the first ten branches, only. Recall that the first design did not take into account any parametric uncertainty. Hence the nominal performance is better than the open-loop; however, 10% parametric uncertainty can cause a deviation more than twice the nominal z_0 . In the second design, by augmenting the exogenous inputs w with the first-order effect of the parametric changes, a more cautious nominal design is achieved. With uncertainty in the first ten parameters, the worst-case deviation is now half of open-loop deviation, although the nominal performance is slightly worse than the first nominal design.

6 Further Robustness Analysis

A little more notation is needed for this section. For $A \in \mathbb{R}^{n \times n}$, $\rho_{\mathbb{R}}(A)$ denotes the maximum absolute value of the real eigenvalues of A . For a real matrix A , $|A|$ denotes the absolute value of A , i.e., $e_i^T \mid A \mid e_j = \mid e_i^T A e_j \mid$. $\Pi(A) = \rho_{\mathbb{R}}(\mid A \mid) = \rho(\mid A \mid)$; also referred to as the Perron eigenvalue of A . Let $\mathbb{1} \in \mathbb{R}^n$ denote a vector of all 1's .

Let $H_{zw}(\Delta) = H_{11} + H_{12}\Delta(I - H_{22}\Delta)^{-1}H_{21}$, where $H = \begin{bmatrix} H_{11} & H_{12} \\ H_{21} & H_{22} \end{bmatrix} \in \mathbb{R}^{(n_z+n_\delta)\times(n_w+n_\delta)}$ and Δ is diagonal. Under these assumptions,

$$\min_{\substack{\|H_{zw}(\Delta)\|_{i,\infty} \leq \gamma \\ \|\Delta\|_{i,\infty} \leq \frac{1}{\gamma} \\ \det(I - H_{22}\Delta) \neq 0}} \gamma$$

$$= \max_{\substack{e \in \{e_1,\dots,e_{n_z}\} \\ w \in \{-1,1\}^{n_w} \\ S \in \mathrm{diag}\{-1,1\}^{n_\delta}}} \rho_{\mathbb{R}} \left(\begin{bmatrix} e^T H_{11} w & e^T H_{12} \\ H_{21} w & H_{22} \end{bmatrix} \begin{bmatrix} 1 & 0 \\ 0 & S \end{bmatrix} \right)$$

$$\leq \max_{\substack{e \in \{e_1,\dots,e_{n_z}\} \\ w \in \{-1,1\}^{n_w}}} \Pi \left(\begin{bmatrix} e^T H_{11} w & e^T H_{12} \\ H_{21} w & H_{22} \end{bmatrix} \right)$$

$$\leq \max_{1 \leq i \leq n_z} \Pi \left(\begin{bmatrix} e_i^T \mid H_{11} \mid \mathbb{1} & e_i^T H_{12} \\ \mid H_{21} \mid \mathbb{1} & H_{22} \end{bmatrix} \right)$$

$$\leq \left\| \begin{bmatrix} H_{11} & H_{12} \\ H_{21} & H_{22} \end{bmatrix} \right\|_{i,\infty} .$$

A cheap lower bound to the optimal γ value above can be obtained by evaluating $\rho_{\mathbb{R}}$ of a smaller number of matrices rather than the huge number $(n_z 2^{(n_w+n_\delta)})$. Note that typically, $n_\delta \gg n_w$. Using the Perron eigenvalues, coarser upper bounds on the optimal γ can be obtained by $n_z 2^{n_w}$ and n_z eigenvalue evaluations, respectively.

Note also that if the entries of H are all positive, then the optimal γ is given by

$$\min_{\substack{\|H_{zw}(\Delta)\|_{i,\infty} \leq \gamma \\ \|\Delta\|_{i,\infty} \leq \frac{1}{\gamma} \\ \det(I - H_{22}\Delta) \neq 0}} \gamma = \max_{1 \leq i \leq n_z} \Pi \left(\begin{bmatrix} e_i^T H_{11} \mathbb{1} & e_i^T H_{12} \\ H_{21} \mathbb{1} & H_{22} \end{bmatrix} \right).$$

7 Conclusion

The sensitivity and robustness to parameter uncertainty of operating points of thermal processes has been investigated using static feedforward/feedback control. The problem is motivated using a large-scale linear resistive network. Efficient computational tools are developed to handle a large number of nodes and branches. Successive design studies involving different operating points, actuator/sensor selections can be easily performed.

References

[1] L. O. Chua and P. Lin, *Computer-Aided Analysis of Electronic Circuits: Algorithms and Computational Techniques*, Prentice-Hall, 1975.

[2] F. P. Incropera and D. P. DeWitt, *Introduction to Heat Transfer*, John Wiley & Sons, 1985.

[3] Yu. Nesterov and A. Nemirovsky, *Interior Point Polynomial Methods in Convex Programming: Theory and Applications*, SIAM, 1993.

[4] L. Vandenberghe and S. Boyd, "Primal-dual potential reduction method for problems involving matrix inequalities," submitted to Math. Programming, 1993.